Practical delay modeling of externally recirculated burned gas fraction for Spark-Ignited engines

Delphine Bresch-Pietri, Thomas Leroy, Jonathan Chauvin and Nicolas Petit

Abstract In this chapter, the authors provide an overview and study of the low-pressure burned gas recirculation in spark-ignited engines for automotive powertrain. It is shown, at the light of supportive experimental results, that a linear delay system permits to capture the dominant effects of the system dynamics. The modeled transport delay is defined by implicit equations stemming from first principles and can be calculated online. This model is shown to be sufficiently accurate to replace a sensor that would be difficult and costly to implement on commercial engines.

1 Introduction

In this chapter, the authors focus on an application problem in the area of automotive powertrain control . Indeed, in the past decades, the still more stringent norms on fuel consumption and pollutant emissions for automotive engines have substantially increased the architecture of thermal engines and, consequently, the complexity of the control task. In this context, the treatment of time-delay systems constitutes an important design consideration, as delays are an often encountered phenomenon in powertrain systems, as highlighted by numerous studies [9].

Delphine Bresch-Pietri
Department of Mechanical Engineering, Massachussetts Institute of Technology, 77 Massachussetts Avenue, Cambridge MA 02139, USA e-mail: dbp@mit.edu

Thomas Leroy and Jonathan Chauvin
IFP Energies nouvelles, Département Contrôle, Signal et Système, 1 et 4 avenue du Bois-Préau, 92852 Rueil-Malmaison, France e-mail: thomas.leroy@ifpen.fr, jonathan.chauvin@ifpen.fr

Nicolas Petit
MINES Paristech, Centre Automatique et Systèmes, Unité Mathématiques et Systèmes, 60 Bd St-Michel, 75272 Paris, Cedex 06 France e-mail: nicolas.petit@mines-paristech.fr

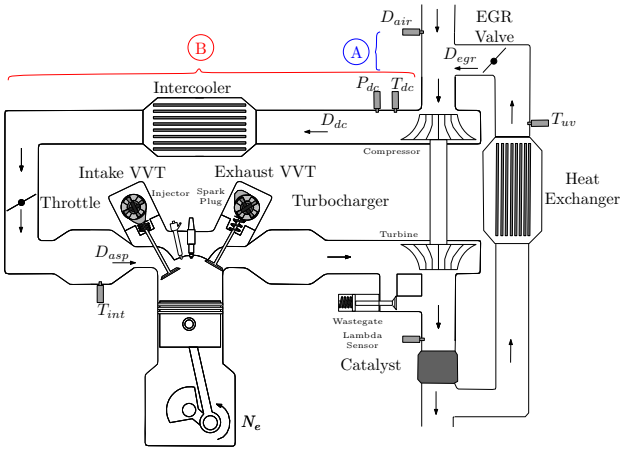

Fig. 1 Scheme of a turbocharged SI engine equipped with direct injection, VVT and a low-pressure EGR loop.

In this chapter, the particular application under consideration is exhaust gas recirculation (EGR) through a low-pressure (LP) circuit for a Spark-Ignited (SI) engine. It is shown in this chapter that this technology introduces a significant delay transport which should be taken into account to accurately estimate and control the (distributed) composition of the gas inside the intake line. Before detailing this point, a few elements of context are given to motivate the use of EGR.

1.1 Why exhaust gas recirculation ?

One of the main issues when dealing with downsized[1] SI engine is the prevention of the malicious knock phenomenon. This unwanted self-ignition of the gaseous mixture which appears at high load, due to high resulting thermodynamical conditions, may cause the engine to stall and eventually damage the combustion chamber.

One of the solutions considered in the automotive industry to handle this phenomenon consists in using EGR through a low-pressure circuit [8, 18]. In such a configuration, exhaust burned gas are picked up downstream of the catalyst and reintroduced upstream of the compressor. A typical implementation is represented in Fig. 1. Indeed, the addition of exhaust gas into the gaseous blend leads to an increase of the auto-ignition delay: intermixing the incoming air with recirculated exhaust gas dilutes the mixture with inert gas, increases its specific heat capacity and, consequently, lowers the peak combustion temperature. Then, the net effect of

[1] Downsizing consists in the reduction of the engine size to operate on more efficient points. To provide similar performances to much larger engines, these engines are usually equipped with a turbocharger and direct injection devices. This technology has appeared in the last decade as a major solution to reduce fuel consumption [14].

EGR is a prevention of knock which leads to potential substantial improvements of overall combustion efficiency [6].

1.2 Necessity of a virtual composition sensor

Yet, EGR has some downsides. During tip-outs (defined as a transient mode during which the torque demand is suddenly decreased), the presence of burned gases in the intake manifold and later in the combustion chamber seriously impacts the combustion process and may cause the engine to stall. Further, EGR has strong interactions with simultaneously operating engine controllers such as the regulation of Fuel-to-Air Ratio (FAR) to stoichiometry (see [9]) or the spark advance. Indeed, EGR impacts the fresh air quantity which is aspirated inside the cylinder at each stroke. Therefore, to counteract the impact of intake burned gas, a solution would be to modify the feedforward action on the cascaded controllers (fuelpath controller and ignition path controller) based on a real-time estimate $\hat{x}$ of the intake burned gas rate. Nevertheless, no real-time sensor of this variable is embedded in any real-world vehicle and obtaining such an estimate is not an easy task. The approach that we advocate here is to substitute one such sensor with a model[2].

For the considered low-pressure gas recirculation circuit, the amount of reintroduced burned gases is controlled by the EGR Valve, an actuator which is located upstream of the compressor. Consequently, the relative long distance between the compressor and the inlet manifold leads to a large transport delay (up to several seconds depending on the engine specifications). Most importantly, this delay depends on the gas flow rate and therefore is time-varying to a large extent.

1.3 Comparison with Diesel EGR

In the seemingly similar context of automotive Diesel engines[3], numerous solutions for the discussed control issues have been developed in the last decades (see for example [1, 21, 23] and the references therein). Yet, none of these strategies includes a transport delay model, which as has been discussed is non-negligible for SI engines. Indeed, on top of using a low-pressure EGR circuit configuration (which substantially increases the transport lag compared to high-pressure configuration studied in [12, 20]), SI engines combustion constraints significantly increase the scale of the delay: (i) first, SI engines operations require a stoichiometric FAR, which results into a fraction of burned gas close to one in the exhaust line. Consequently, to obtain a given intake fraction of burned gas, the amount of exhaust burned gas to be

[2] Other works (see [5]) investigate the potential of using a cylinder pressure sensor signal. Yet, due to stringent cost constraints, such a sensor is not currently commercially embedded.

[3] The use of EGR for Diesel engines has been widely investigated for a different purpose, to decrease the emissions of nitrogenous oxides emissions.

reintroduced at steady state is substantially lower than the corresponding one for Diesel engines; (ii) besides, on the contrary of Diesel engines, SI engines may operate at intake pressure under atmospheric values (low loads). Then, on this operating range, the steady-state gas flow rates are considerably less important.

For these reasons, modeling this transport delay is a milestone in the design of controllers for SI engines.

In this chapter, a model of the intake burned gas rate is presented, accounting explicitly for transport time-varying delay and its dependency on the history of gas flow rates in a way which compensates for thermal exchanges and induced gas velocity changes. It is then used as a "software" sensor. This estimation is based on a practical delay calculation methodology which is experimentally validated on a test bench. The purpose of this chapter, based on the previous contribution [4], is to present this model along with its practical validation, to enhance the role of the variable transport delay in the modeling and to illustrate how this estimate can be used to coordinate the controllers. Experimental FAR control tests stress the relevance of the estimate.

This chapter is organized as follows. In Section 2, we present a model of the intake burned gas rate dynamics, under the form of a linear time-varying system with a time-dependent delay output. The practical usage of this model is discussed. Implementation and experimental results are provided in Section 3. We conclude by briefly sketching potential directions of work for combustion control improvements.

2 Modeling

Consider the airpath of a turbocharged SI engine equipped with intake throttle, wastegate, dual independent VVT actuators and a low-pressure external gas recirculation (EGR) loop as depicted in Fig. 1. Such a setup is usually considered for downsized engines (see [10]). Acronyms and notations used below are listed in Table 1.

Formally, the in-cylinder burned gas fraction x_{cyl} is defined as the ratio between the in-cylinder burned gas mass originated from the EGR loop m_{bg} and the total mass of gas in the cylinder volume $m_{asp} = m_{air} + m_{bg}$ in which m_{air} is the aspirated mass of fresh air, i.e.

$$x_{cyl} = \frac{m_{bg}}{m_{air} + m_{bg}}$$

From now on, this variable is considered equal to x the intake burned gas fraction [4].

[4] Actually, this relation depends mainly on the VVT control strategy. We neglect this influence here for sake of clarity.

2.1 Dilution Dynamics and transport delay

Defining x_{lp} as the burned gas rate upstream of the compressor, the EGR dynamics can be expressed in terms of the mass flow rates of air D_{air} and recirculated burned gas D_{egr} as

$$\dot{x}_{lp} = \alpha \left[-(D_{egr}(t) + D_{air}(t))x_{lp}(t) + D_{egr}(t) \right] \quad (1)$$

$$x(t) = x_{lp}(t - \tau(t)) \quad (2)$$

where $\tau(t)$, the delay between this ratio and the intake composition, can be implicitly defined according to the integral equation (Plug-Flow assumption for the gas composition along the intake line, see [16])

$$\int_{t-\tau(t)}^{t} v_{gas}(s)ds = L_P \quad (3)$$

where L_P is the pipe length from the compressor down to the intake manifold and v_{gas} stands for the gas velocity.

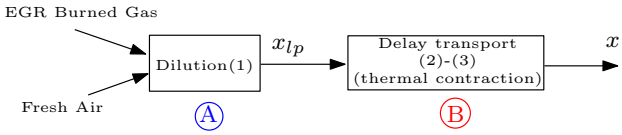

Fig. 2 Scheme of the intake burned gas fraction dynamics.

Equation (1) is a balance equation on the volume downstream of the EGR valve, using the fact that the EGR circuit is totally filled with burned gas[5]. Depending on engine setups, the thermodynamics constant α appearing in (1) is either measured or known.

The integral delay model (3) is representative of a wide class of systems involving transport phenomena [2, 17, 22]. This delay can be understood as a propagation time for a variable velocity v_{gas}. In particular, one can observe that at steady-state this delay is inversely proportional to the gas speed, which is a more intuitive modeling one can think of. Alternatively, PDE models can be used to represent more accurately the induced transport dynamics. However, the induced computational burden discard them from real-time implementation.

In a nutshell, following the proposed model, which is pictured in Fig. 2, the intake burned gas fraction is the result of a first order dynamics coupled with a transport delay.

[5] For SI engines, the FAR is regulated to its stoichiometric value (see [7]), which results into an exhaust burned gas fraction close to unity.

For sake of clarity, the approach used to model the mass flow rate quantities (D_{egr},...) used through (1)-(3) is not detailed here and given in Appendix. Using the approach presented in Appendix, one can now assume that they are known quantities. To provide an implementable open-loop estimate of x based on the model (1)-(3), a practical calculation methodology of the delay τ, using only real-time measurements, remains to be developed. This point is now addressed.

2.2 Transport delay description

Equation (3) implicitly determines the delay according to the gas speed along the intake line, which, on top of being a distributed parameter, is not measured in practice. Further, the thermodynamical transformations the gas is submitted to in the intake line modify this distributed velocity. This complexity can be handled by a relatively fair delay description.

Indeed, using the ideal gas law (as is classically done for engine gas flows, e.g. in [7]), one can relate this speed to current thermodynamical conditions and mass flow rates, which are measured/modeled. Namely,

$$\forall t \geq 0\,, \quad v_{gas}(t) = \frac{1}{S(t)} \frac{rT(t)}{P(t)} \left[D_{air}(t) + D_{egr}(t)\right]$$

where S is the current pipe area, T, P are the current temperature and pressure values, r is, as previously, the (common) ideal gas constant of both fresh air and burned gas. In practice, the total mass flow rate which appears under the integral is estimated as $D_{air}(s) + D_{egr}(s) = D_{dc}(s)$ (a model of the mass flow rate D_{dc} is provided in (7) in Appendix).

A thermal contraction of the gas occurs inside the intake cooler, resulting in spatial changes of the gas velocity v_{gas}. To model this, we split the intake line into three main sections with three respective and cumulative transport delays τ_1, τ_2 and τ_3 such that $\tau = \tau_1 + \tau_2 + \tau_3$. This decomposition, pictured in Fig. 3, is as follows:

- *downstream of the compressor to the intercooler :* in this part, the current pressure and the temperature are measured and one can write

$$\int_{t-\tau_1(t)}^{t} \frac{rT_{dc}}{P_{dc}} D_{dc}(s)ds = V_1 \tag{4}$$

  with V_1 the corresponding volume.
- *inside the intercooler:* considering boundary conditions, the pressure inside the intercooler can reasonably be assumed as constant and equal to the input one P_{dc}. Further, we assume that the spatial profile of the inside temperature is affine with respect to the spatial variable, with measured boundary conditions T_{dc} and T_{int}[6]. Under this assumption, equation (3) can be reformulated on this section as

[6] i.e. $T(x) = \frac{T_{int} - T_{dc}}{L_2} x + T_{dc}$

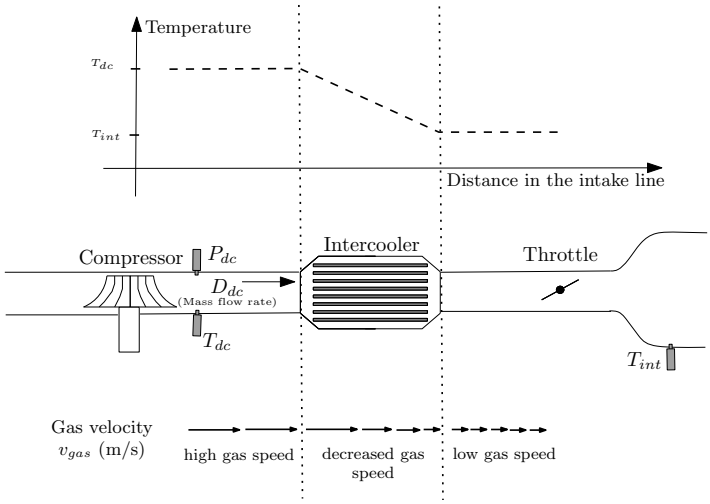

Fig. 3 The intake line is split into three parts to account for the spatial differences of the gas velocity. The temperature decreases, which results into an increase of velocity which is analytically determined by the ideal gas low fed with measurements from temperature and pressure sensors located along the line.

$$\int_{t-\tau_2(t)-\tau_1(t)}^{t-\tau_1(t)} \frac{r}{P_{dc}} D_{dc}(s)ds = S_2 \int_0^{L_2} \frac{dx}{T(x)} = \frac{V_2}{T_{int}-T_{dc}} \ln\left(\frac{T_{int}}{T_{dc}}\right) \tag{5}$$

where L_2, S_2 and V_2 are the corresponding length, area and volume.

- *downstream of the intercooler to the intake manifold:* in this section, the temperature can be approximated by the intake manifold temperature, which yields

$$\int_{t-\tau_3(t)-\tau_2(t)-\tau_1(t)}^{t-\tau_2(t)-\tau_1(t)} \frac{rT_{int}}{P_{dc}} D_{dc}(s)ds = V_3 \tag{6}$$

with V_3 the corresponding volume.

Knowing intermediate volumes V_1, V_2 and V_3, one can calculate the delay in a very straightforward manner, solving, one after the other, (4), (5) and finally (6). The transport delay is then simply deduced as $\tau(t) = \tau_1(t) + \tau_2(t) + \tau_3(t)$.

The involved numerical solving is based on the observation that the integrand is strictly positive and that the integral is then an increasing function of the delay τ_i ($i \in \{1,2,3\}$) appearing in its lower bound. Then, by simply sampling and evaluating the integral at increasing values of τ_i starting from 0, one can obtain a numerical evaluation of the corresponding delay. All these calculations are on-line compliant[7].

[7] This approach is directly inspired of [17] for modeling plug flows in networks of pipes problem.

2.3 Estimation strategy with practical identification procedure

An estimation strategy of the model above is summarized on Fig. 4. Real-time measurements of temperatures and pressures serve to determine the value of the delay. These information are commonly available using (cheap) embedded sensors. Values for physical volumes (V_{lp}, V_1, V_2 and V_3) can be used to calibrate the model.

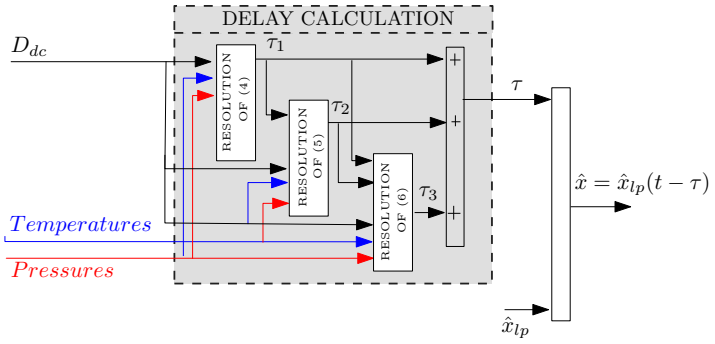

Fig. 4 Scheme of the proposed delay calculation strategy for intake burned gas fraction estimate x. The numerical solving of implicit integral equations (4)-(6) can be obtained by sampling and calculating the integrals at increasing values of τ_i starting from 0, which are real-time compliant calculations.

It is worth noticing that splitting the intake line as has been proposed in the previous section has been motivated mainly by the engine embedded instrumentation and in particular by the availability of temperature (and pressure) sensors. It can be easily adapted to any considered engine. In particular, if no temperature and no pressure sensors are available downstream of the compressor, they can be efficiently approximated by the intake ones at the expense of slight updates of the volumes values in the fit. Indeed, the two pressures are sufficiently close and these equations are of moderate temperature sensitivity. In such a case, the delay can be directly determined by one equation of type (4).

3 Experimental results

The proposed model is now used as a “software” sensor. The obtained estimate is embedded into a real-time control target and employed at test-bench. The experiments aim at validating the model presented in Section III and in particular the delay modeling.

3.1 Experimental setup and indirect validation methodology from FAR measurements

The engine under consideration is a 1.8L four cylinder SI engine with direct injection (see [13] for details). The airpath consists of a turbocharger controller with a wastegate, an intake throttle, an intercooler and a LP-EGR loop. This engine setup is consistent with the scheme reported in Fig. 1.

To validate the proposed estimation strategy, as *no real-time information of the intake burned gas fraction is available* for this engine, we focus on the open-loop response of the normalized FAR. This quantity is formally defined in terms of the fuel and fresh air mass aspirated inside the cylinder at each stroke as $\phi = \frac{1}{FAR_{st}} \frac{m_{inj}}{m_{air}}$. It has to be regulated to the unity to maximize the efficiency of after-treatment devices. Usually, this control is realized with the injection path[8], using the measurements of a dedicated sensor located downstream of the turbine (Lambda Sensor).

Here, the FAR is simply controlled by a feedforward strategy on the mass of fuel injected in the cylinder, namely

$$m_{inj} = FAR_{st} m_{air}$$

The additional feedback term that is usually used is purposely omitted.

When no burned gas is recirculated, the in-cylinder air mass is accurately estimated with the model presented in Appendix (see [15]), i.e. $m_{air} = m_{asp}$. When burned gas are reintroduced, one can formally write $m_{air} = m_{asp} - m_{bg} = m_{asp}(1-x)$ and, consequently, estimate the in-cylinder air mass as $m_{asp}(1-\hat{x})$ where $\hat{x}$ is the intake burned gas fraction estimate provided by the proposed model.

With this setup, it is possible *to qualitatively relate the FAR variations to the intake burned gas fraction*. Indeed, if the estimation is accurate, the normalized FAR remains close to unity and, in turn, one then obtains an indirect validation of the intake burned gas rate estimation. Any offset reveals a steady-state estimation error while any temporary undershoot (or overshoot) reveals a mis-estimation of the delay.

3.2 First validation : variation of the amount of reintroduced EGR (constant delay)

The first scenario under consideration here is a variation of the amount of reintroduced burned gas for a given operating point : constant engine speed $N_e = 2000$ rpm for a requested torque of 12.5 bar. This scenario is of particular interest for validation as the intake mixture composition is the only varying variable.

[8] the airpath being then dedicated to meet torque requests.

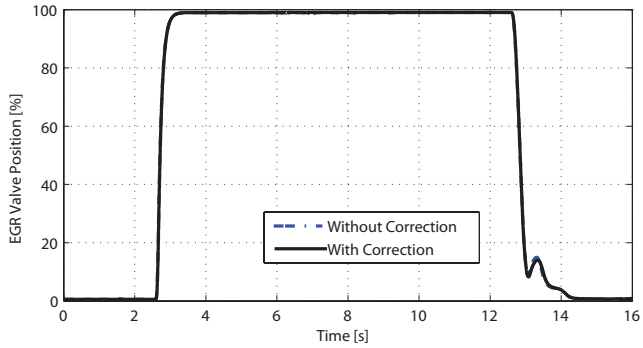

(a) EGR Valve position

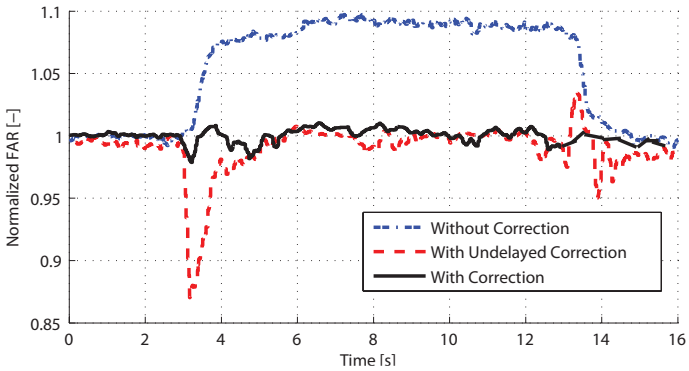

(b) Normalized FAR

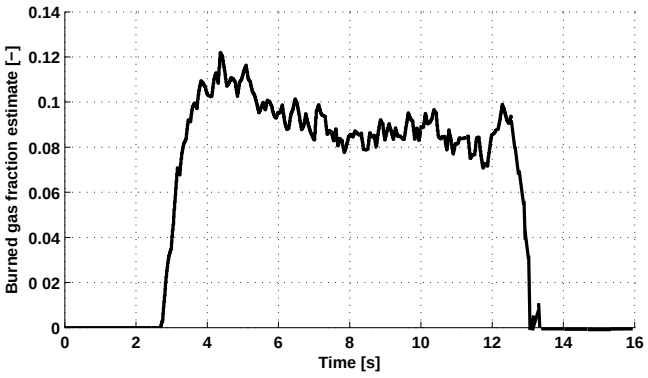

(c) Burned gas fraction estimate

Fig. 5 Experimental results for constant engine speed ($N_e = 2000$ rpm) and torque request ($IMEP = 8$ bar). The EGR valve position is pictured in (a). Blue dotted curve : gas composition transient without estimation. Black curve : gas composition transient with estimation and feedforward correction.

Fig.5(c) pictures the intake burned gas fraction estimates corresponding to the EGR valve variations pictured in (a). The corresponding delay is constant and simply not reported.

With burned gas feedforward correction, i.e. considering $m_{air} = (1-\hat{x})m_{asp}$
The corresponding normalized FAR evolution is pictured in black, in Fig.5(b). One can easily observe that the normalized FAR remains satisfactorily close to the unity. This behavior reveals a good fit between the real intake manifold burned gas rate and the estimate one provided in Fig.5(c).

For sake of comparisons, the FAR response with a burned gas fraction estimate computed neglecting the delay is also provided (red dotted curves). Neglecting the delay leads to a transient overestimation of the burned gas fraction and, consequently, to a significant FAR undershoot. This stresses the importance of the delay into the burned gas rate dynamics and the relevance of the proposed model.

Without burned gas correction, i.e. considering $m_{air} = m_{asp}$
In that case, as the in-cylinder mass air is overestimated, the injected mass of fuel turns to be too large. This results into a deviation of the normalized FAR up to 1.09 (blue dotted curve in Fig.5). A feedback control would reasonably eliminate this offset, but, as the obtained FAR measurement is delayed (see [3, 11] for a FAR dynamics details), an important overshoot would still be present.

3.3 Second validation : torque transients (varying delay)

The second scenario under consideration is a torque transient requested by the driver, a step from 6 bar to 12.5 bar. This tip-in is a typical driving situation case study, which defines an increase in the in-cylinder air mass set point and consequently on the total gas flow rate. Then, both dilution dynamics (1) and the delay are varying.

Further, this also implies a variation of the requested amount of reintroduced burned gas, as the initial operating point is low loaded and does not require any EGR. Without dedicated control structure, we simply consider here the EGR valve position either fully closed or fully opened. Its variations are pictured in Fig. 6(c).

The corresponding calculated delay is given in Fig. 6(d). As the total mass flow rate increases during the transient, the delay decreases, as expected.

Finally, as in the previous scenario, the FAR remains close to the unity. This validates the burned gas fraction estimate variations depicted in Fig. 6(b).

4 Conclusion and perspectives

In this chapter, it has been shown that low-pressure burned gas recirculation for SI engines can be accurately represented as a first order linear dynamics with a time-varying delay. The value of the delay is determined by an implicit integral relation

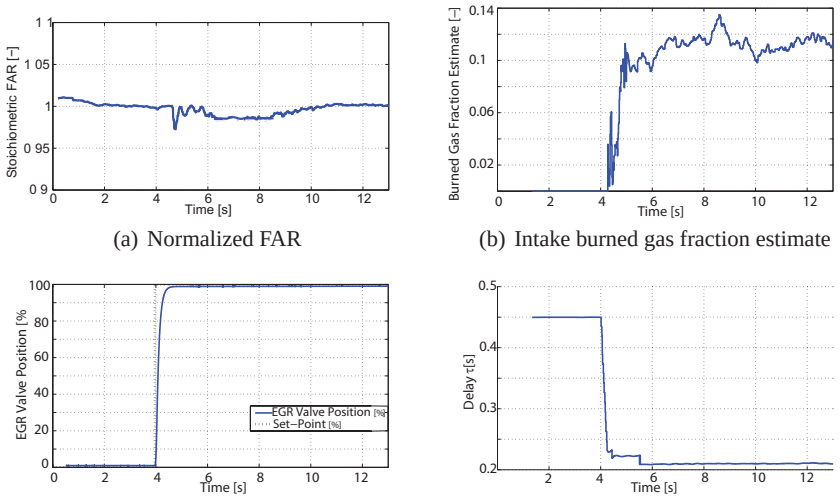

(a) Normalized FAR (b) Intake burned gas fraction estimate

(c) EGR valve position (d) Transport delay

Fig. 6 Experimental results for constant engine speed ($N_e = 2000$ rpm) and transient torque request (step from $IMEP = 6$ bar to 12.5 bar), resulting into a delay variation. The normalized FAR response pictured in (a) uses the intake burned gas fraction estimation pictured in (b), obtained with the on-line estimation of the delay (d).

in which data from commonly available sensors (temperatures, pressures) come into play through the ideal gas law. Experiments conducted at test bench validate both this model and the proposed delay calculation methodology and highlight the key rule played by the delay in the overall dynamics.

This result opens new perspectives in term of engine control applications : coordination of low-level controllers, advanced feedforward compensation (FAR, Spark Advance),... Yet, because the delay is varying, new techniques are required, especially if one wishes to take advantage of the known source of delay variability.

In particular, the input-dependency of the delay brings new challenges in term of control. As mentioned in [19], while a few number of works have investigated open-loop tracking for input-dependent delay systems, closed-loop control is still an open problem.

Appendix : Flow rates model

In-cylinder and downstream compressor mass flow rates

We use the model of in-cylinder gas mass presented in [15] to define mass flow rates. In this model, D_{asp} is represented as a function of the engine speed N_e, the manifold pressure P_{int} and the intake and exhaust VVT actuators positions. Using the ideal gas law, this flow rate is dynamically related to the flow rates through the

throttle and downstream of the compressor as

$$D_{thr} = D_{asp}(N_e, P_{int}, VVT) + \frac{V_{int}}{rT_{int}}\dot{P}_{int}\,, \quad D_{dc} = D_{thr} + \frac{V_P}{rT_{dc}}\dot{P}_{dc} \tag{7}$$

where $r = r_{air} = r_{bg}$ is the (common) ideal gas constant. The variables used in these two last equations are either known or measured.

EGR mass flow rate Assuming that an intake mass air flow sensor is available on the engine, only the mass flow rate D_{egr} remains to be expressed. Neglecting the mis-synchronization of the flows signals, we simply write (with a projection operator forcing the flow rate to be zero when the valve is closed)

$$\hat{D}_{egr}(t) = \text{Proj}_{\theta_{egr}>0}\{D_{dc}(t) - D_{air}(t)\}$$

Table 1 Nomenclature

Notations					
Symbol	**Unit**	**Description**	**Symbol**	**Unit**	**Description**
D_{air}	kg/s	Air mass flow rate upstream of the compressor	V_P	m^3	Pipe volume from the compressor to the intake manifold
D_{egr}	kg/s	EGR mass flow rate through the EGR valve	r	J/kg/K	Specific ideal gas constant
D_{dc}	kg/s	Mass flow rate downstream of the compressor	L_P	m	Pipe length from the compressor to the intake manifold
D_{asp}	kg/s	In -cylinder mass flow rate	θ_{egr}	%	EGR Valve Position
v_{gas}	m/s	Gas speed	m_{air}	mg/str	In-cylinder air mass
T_{dc}	K	Temperature downstream of the compressor	m_{bg}	mg/str	In-cylinder burned gas mass
P_{dc}	Pa	Pressure downstream of the compressor	m_{asp}	mg/str	In-cylinder total gas mass
T_{atm}	K	Atmospheric temperature	m_{inj}	mg/str	Injected mass of fuel
P_{atm}	Pa	Atmospheric pressure	FAR_{st}	-	Stoichiometric FAR
V_{lp}	m^3	Volume between the EGR valve and the compressor	x	-	Intake burned gas fraction
			x_{lp}	-	Burned gas fraction upstream of the compressor
			x_{cyl}	-	In-cylinder burned gas fraction

Acronyms	
EGR	Exhaust Gas Recirculation
FAR	Fuel-to-Air Ratio
IMEP	Indicated Mean Effective Pressure
SI	Spark Ignited

References

1. M. Ammann, N. P. Fekete, L. Guzzella, and A. H. Glattfelder. Model-based control of the VGT and EGR in a turbocharged common-rail Diesel engine: theory and passenger car implementation. *SAE transactions*, 112(3):527–538, 2003.
2. D. Bresch-Pietri. *Robust control of variable time-delay systems. Theoretical contributions and applications to engine control.* PhD thesis, MINES ParisTech, 2012.

3. D. Bresch-Pietri, J. Chauvin, and N. Petit. Adaptive backstepping controller for uncertain systems with unknown input time-delay. application to SI engines. In *Proc. of the Conference on Decision and Control*, 2010.
4. D. Bresch-Pietri, T. Leroy, J. Chauvin, and N. Petit. Practical delay modeling of externally recirculated burned gas fraction for Spark-Ignited engines. In *Proc. of the 11th IFAC Workshop on Time-Delay Systems*, 2013.
5. M. A. R. Caicedo, E. Witrant, O. Sename, P. Higelin, et al. A high gain observer for enclosed mass estimation in a spark ignited engine. In *Proceedings of the 2012 American Control Conference*, 2012.
6. A. Cairns and H. Blaxill The effects of combined internal and external gas recirculation on gasoline controlled auto-ignition. In *Proc. of the Society of Automotive Engineering World Congress*, number 2005-01-0133, 2005
7. J. B. Heywood. *Internal combustion engine fundamentals*. McGraw-Hill New York, 1988.
8. B. Hoepke, S. Jannsen, E. Kasseris, and W. K. Cheng. EGR effects on boosted SI engine operation and knock integral correlation. *SAE International Journal of Engines*, 5(2):547–559, 2012.
9. M. Jankovic and I. Kolmanovsky. Developments in control of time-delay systems for automotive powertrain applications. In *Delay Differential Equations, recent advances and new directions, Balachandran, B. and Kalmar-Nagy, T. and Gilsinn D. E.*, pages 55–92. Springer Science, 2009.
10. U. Kiencke and L. Nielsen. *Automotive control systems*. Springer-Verlag, Berlin, 2000.
11. J. Lauber, T. M. Guerra, and M. Dambrine. Air-fuel ratio control in a gasoline engine. *International Journal of Systems Science*, 42(2):277–286, 2011.
12. J. Lauber, T. M. Guerra, and W. Perruquetti. IC engine: tracking control for an inlet manifold with EGR. *SAE Transactions Journal of Passenger Cars electronic and electrical systems*, 20:913–917, 2002.
13. G. Le Solliec, F. Le Berr, G. Colin, G. Corde, and Y. Chamaillard. Engine control of a downsized spark ignited engine : from simulation to vehicle. In *Proc. of ECOSM Conference*, 2006.
14. B. Lecointe and G. Monnier. Downsizing a gasoline engine using turbocharging with direct injection. In *Proc. of the Society of Automotive Engineering World Congress*, number 2003-03-0542, 2003
15. T. Leroy, J. Chauvin, F. Le Berr, A. Duparchy, and G. Alix. Modeling fresh air charge and residual gas fraction on a dual independant variable valve timing SI engine. *SAE International Journal of Engines*, 1(1):627–635, 2009.
16. R. H. Perry, D. W. Green, and J. O. Maloney. *Perry's chemical engineers' handbook*, volume 7. McGraw-Hill New York, 1984.
17. N. Petit, Y. Creff, and P. Rouchon. Motion planning for two classes of nonlinear systems with delays depending on the control. In *Proceedings of the 37th IEEE Conference on Decision and Control*, pages 1007–1011, 1998.
18. S. Potteau, P. Lutz, S. Leroux, S. Moroz, et al. Cooled EGR for a turbo SI engine to reduce knocking and fuel consumption. In *SAE Technical Paper*, pages 01–3978, 2007.
19. J.-P. Richard Time-delay systems; an overview of some recent advances and open problems. In *Automatica*, 39:1667-1694, 2003.
20. A. Stotsky and I. Kolmanovsky. Application of input estimation techniques to charge estimation and control in automotive engines. *Control Engineering Practice*, 10(12):1371–1383, 2002.
21. M. J. Van Nieuwstadt, I. V. Kolmanovsky, P. E. Moraal, A. Stefanopoulou, and M. Jankovic. EGR-VGT control schemes: experimental comparison for a high-speed diesel engine. *Control Systems Magazine, IEEE*, 20(3):63–79, 2000.
22. K. Zenger and A. J. Niemi. Modelling and control of a class of time-varying continuous flow processes. *Journal of Process Control*, 19(9):1511–1518, 2009.
23. M. Zheng, G. T. Reader, and J. G. Hawley. Diesel engine exhaust gas recirculation–a review on advanced and novel concepts. *Energy Conversion and Management*, 45(6):883–900, 2004.